Theoretical investigation and computational evaluation of overtone and combination features in resonance Raman spectra of polyenes and carotenoids

Matteo Tommasini,[a,b]* Giovanna Longhi,[c,d] Sergio Abbate[c,d] and Giuseppe Zerbi[a]

Introduction

The resonant Raman spectra of several carotenoids were investigated in the past, and overtone and combination bands were assigned[1]; all of the latter involve intense CC stretching modes related with the effective conjugation coordinate (ECC, also denoted with $\mathcal{R}$; for details, see the work of Castiglioni *et al.*[2] and the references therein). The data reported by Okamoto *et al.*[1] reveal that mechanical anharmonicity is little, as one expects for vibrations involving the π-conjugated backbone of carotenoids; however, it is noteworthy that in the work of Okamoto *et al.*,[1] so many overtone and combination data were made available, in that a full set of principal and cross anharmonicity constants χ_{ii} and χ_{ij} were derived from experimental frequencies with great accuracy. Their values were found in the range 1–5 cm^{-1}. In this work, we focus our attention on the second relevant aspect of overtones and combinations in Raman spectroscopy: the intensities, which were not discussed in the work of Okamoto *et al.*[1] and are usually neglected also in the analysis of off-resonance Raman spectra, because of their weak signal. Indeed, we notice that the ν^4-dependence of Raman intensities hampers observation of overtones, as noted, e.g. by Henry *et al.* in their local mode studies.[3] We will tackle this problem by studying, in resonance conditions, the scattering tensor, which directly determines the intensity of higher-order Raman transitions.

The calculation of off-resonance Raman spectra of carotenoids can be carried out with density functional theory (DFT) methods,[4] and it reveals a good match with the experimental counterpart (see, for instance, the case of β-carotene reported in Fig. 1). This is an encouraging indication that the vibrational dynamics obtained from DFT calculations is a good starting point for successive developments taking into account resonance effects.

It has been shown that in resonance conditions, higher-order Raman scattering processes are significantly enhanced compared with off-resonance conditions.[5] In fact, it is not by chance that it is possible to observe and assign a considerable number of overtones and combinations in the resonant Raman spectra of several carotenoids.[1,4]

The use of $\mathcal{R}$-coordinate[2] has proved to be useful for investigating the possible structure of carotenoid natural pigments[4] and other polyenes of biological interest.[6] [1] On the other hand, the calculation of the Raman scattering tensor of fundamental transitions by following the same theoretical framework here considered[7] was successful for other π-conjugated systems, namely polycyclic aromatic hydrocarbons.[8] In this work, we will show that by joining the theory of $\mathcal{R}$-coordinate[2] with Nafie–Stein–Peticolas theory,[5,7] it is possible to straightforwardly compute the resonant Raman response of β-carotene. In particular, the Raman intensity of each

* *Correspondence to: Matteo Tommasini, Dipartimento di Chimica, Materiali e Ingegneria Chimica, Politecnico di Milano, Piazza Leonardo da Vinci, 32, 20133 Milan, Italy. E-mail: matteo.tommasini@polimi.it*

a *Dipartimento di Chimica, Materiali e Ingegneria Chimica, Politecnico di Milano, Piazza Leonardo da Vinci, 32, 20133, Milan, Italy*

b *Consorzio Interuniversitario per la Scienza e Tecnologia dei Materiali (INSTM), Unità di Ricerca del Politecnico di Milano (Dip. CMIC), Piazza Leonardo da Vinci 32, 20133, Milan, Italy*

c *Dipartimento di Medicina Molecolare e Traslazionale, Università di Brescia, Viale Europa 11, 25123, Brescia, Italy*

d *C.N.I.S.M. Consorzio Interuniversitario Scienze Fisiche della Materia, c/o Università Roma 3, via della Vasca Navale 84, 00146, Rome, Italy*

[1](Because of typographical restrictions, the symbol $\mathcal{R}$ replaces here the symbol commonly used in the previous literature, namely the letter 'ya' of the Cyrillic alphabet).

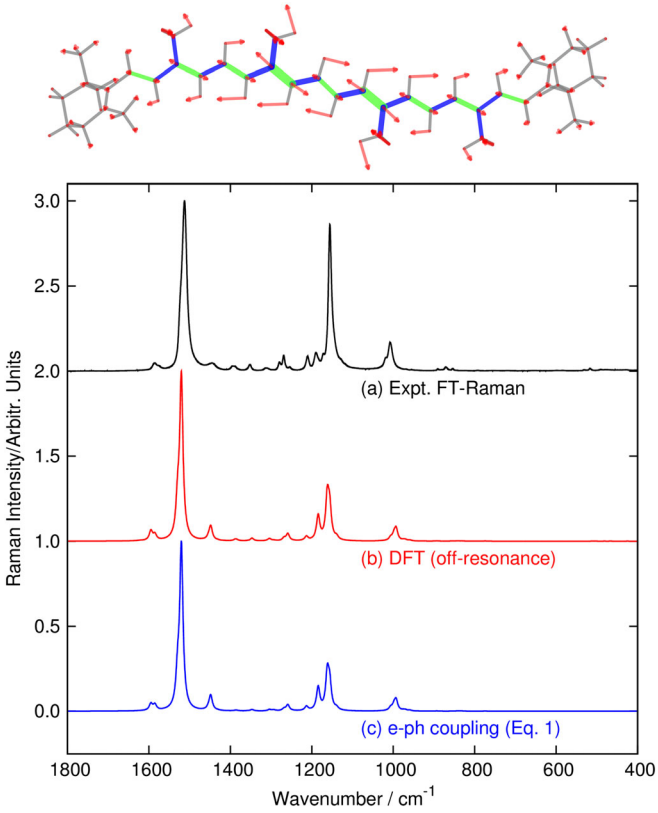

Figure 1. First-order Raman spectrum of β-carotene: comparison of DFT calculations and experiment. Top: representation of the nuclear displacements along the ν_1 normal mode, computed at 1575 cm^{-1}, containing the largest contribution from the $\mathcal{R}$-coordinate (Table 1); the relative stretching/shrinking of CC bonds is indicated with green/blue; red arrows are proportional to the displacement vector of each atom. (a) Experimental off-resonance FT-Raman spectrum (1064 nm excitation, present work); (b) off-resonance Raman spectrum simulated with DFT (B3LYP/6-31G** calculations carried out with Gaussian09[15]); (c) calculated Raman spectrum through Eqn (1): relative intensities proportional to the square of the electron–phonon coupling given by $\mathbf{g}\cdot\mathbf{L}_k$ (see text for details; results from TD-B3LYP/6-31G** calculations). This figure is available in colour online at wileyonlinelibrary.com/journal/jrs

line is the result of the $\mathcal{R}$-coordinate content of the associated normal mode. Furthermore, the extension of this approach to overtones and combinations is feasible thanks to Nafie *et al.*[5] and nicely reveals the role of electron–phonon coupling described by $\mathcal{R}$-coordinate in determining the strength of higher-order Raman processes.

Theoretical model and computations

Electron–phonon coupling

In the present work, we rely on the theory describing the Raman process in terms of time-ordered diagrams, which was introduced in the seventies by Nafie *et al.*[5] to describe interactions of electromagnetic fields and molecules. Such model makes use of a Herzberg–Teller perturbative approach, where a central role is played by the electron–phonon (–vibration) interaction operator $\partial H/\partial Q$. Of particular importance is the diagonal matrix element of the electron–phonon coupling operator, namely $\langle\alpha|\partial H/\partial Q_k|\alpha\rangle$, the term that, at different orders and in resonance condition with excited state $|\alpha\rangle$, is directly responsible for Raman scattering. The calculation of the electron–phonon coupling matrix element with respect to a given excited state can be most conveniently carried out by means of the transformation from normal (Q_k) to Cartesian coordinates (x_i) derivatives, as follows:

$$\left\langle \alpha\left|\frac{\partial H}{\partial Q_k}\right|\alpha\right\rangle = \left\langle \alpha\left|\sum_i \frac{\partial H}{\partial x_i}\frac{\partial x_i}{\partial Q_k}\right|\alpha\right\rangle = \\ = \sum_i \left\langle \alpha\left|\frac{\partial H}{\partial x_i}\right|\alpha\right\rangle L_{ik} = \mathbf{g}\cdot\mathbf{L}_k \tag{1}$$

where normal coordinates are such that $x_i = \sum_k L_{ik}Q_k$. Eqn (1) allows to straightforwardly compute via time-dependent DFT the electron–phonon (e–ph) coupling matrix elements. It suffices to compute the gradient $g_i = \left\langle \alpha\left|\frac{\partial H}{\partial x_i}\right|\alpha\right\rangle$ of the excited state energy surface at the Franck–Condon (FC) point and consider its dot product with the eigenvector L_{ik} of the k-th normal mode under investigation. This can be carried out without any further assumption. This approach is very promising, because, as a first step, we realized that the off-resonance intensities of the Raman fundamental transitions of β-carotene are well reproduced by the squares of the electron–phonon coupling parameters determined with Eqn (1) (Figure 1 and Table 1).

Effective conjugation coordinate theory permits to highlight a further aspect of the electron–phonon coupling related to vibrational displacements. In the space of nuclear coordinates, we can define a peculiar displacement direction, parallel to the gradient $\mathbf{g}$, which is ultimately determined by ECC ($\mathcal{R}$-coordinate). The unit vector $\mathbf{u}_\mathcal{R}$ associated to $\mathbf{g}$ is defined as follows:

$$\mathbf{u}_\mathcal{R} \equiv \frac{\mathbf{g}}{\|\mathbf{g}\|} \tag{2}$$

so that $\mathbf{u}_\mathcal{R}\cdot\mathbf{u}_\mathcal{R} = 1$. The Cartesian nuclear displacements along $\mathcal{R}$ are given by $\mathbf{x} = \mathcal{R}\,\mathbf{u}_\mathcal{R}$. Therefore, by definition, the $\mathcal{R}$-coordinate recovers the strength $\|\mathbf{g}\|$ of the electron–phonon coupling:

$$\left\langle \alpha\left|\frac{\partial H}{\partial \mathcal{R}}\right|\alpha\right\rangle = \left\langle \alpha\left|\sum_i \frac{\partial H}{\partial x_i}\frac{\partial x_i}{\partial \mathcal{R}}\right|\alpha\right\rangle = \\ = \sum_i \left\langle \alpha\left|\frac{\partial H}{\partial x_i}\right|\alpha\right\rangle (u_\mathcal{R})_i = \mathbf{g}\cdot\mathbf{u}_\mathcal{R} = \|\mathbf{g}\| \tag{3}$$

By considering now a given normal coordinate Q_k, whose $\mathcal{R}$ content is denoted $L_{\mathcal{R}k} = \partial\mathcal{R}/\partial Q_k$, we have

$$\left\langle \alpha\left|\frac{\partial H}{\partial Q_k}\right|\alpha\right\rangle = \left\langle \alpha\left|\sum_i \frac{\partial H}{\partial x_i}\frac{\partial x_i}{\partial \mathcal{R}}\frac{\partial \mathcal{R}}{\partial Q_k}\right|\alpha\right\rangle = \\ = \frac{\partial \mathcal{R}}{\partial Q_k}\sum_i \left\langle \alpha\left|\frac{\partial H}{\partial x_i}\right|\alpha\right\rangle \frac{\partial x_i}{\partial \mathcal{R}} = L_{Rk}\,\mathbf{g}\cdot\mathbf{u}_\mathcal{R} \tag{4}$$

Finally,

$$\left\langle \alpha\left|\frac{\partial H}{\partial Q_k}\right|\alpha\right\rangle = \|\mathbf{g}\|L_{\mathcal{R}k} = \left\langle \alpha\left|\frac{\partial H}{\partial \mathcal{R}}\right|\alpha\right\rangle L_{\mathcal{R}k} \tag{5}$$

Equation (5) can be used to provide a physical interpretation of the origin of the Raman scattering activity through electron–phonon coupling. Two important results stem from Eqn (5): The coupling of a given normal mode Q_k to the electronic excited state $|\alpha\rangle$ is proportional to the content $L_{\mathcal{R}k}$ of $\mathcal{R}$ in that mode Q_k. The expectation value over the state $|\alpha\rangle$ of the gradient of H with respect to $\mathcal{R}$ is the key factor of the e–ph coupling and represents its strength.

Table 1. Electron–phonon coupling terms for β-carotene computed through Eqn (1) (TD-B3LYP/6-31G**) compared with off-resonance Raman intensities (B3LYP/6-31G**, last column).

ν_k (cm^{-1})	$\lvert\langle\alpha\rvert\partial H/\partial Q_k\rvert\alpha\rangle\rvert^2$ (%)	I_k (%)	I_k (A^4/amu)
293	0.07	0.08	1 834
872	0.08	0.09	2 026
994	0.19	0.20	4 776
1006	0.28	0.30	7 083
1011	0.16	0.16	3 852
1029	2.98	3.11	73 964
1034	1.42	1.40	33 373
1043	0.87	0.79	18 683
1180	0.65	0.81	19 188
1198	7.04	7.82	186 200
1204	10.31	11.31	269 180
1227	6.48	6.40	152 360
1232	0.16	0.14	3 319
1257	1.18	1.08	25 748
1304	1.71	1.86	44 319
1314	0.57	0.69	16 302
1341	0.26	0.13	3 063
1351	0.38	0.59	14 105
1396	0.35	0.68	16 102
1407	0.05	0.02	553
1435	0.10	0.20	4 820
1438	0.10	0.35	8 401
1483	0.07	0.07	1 722
1500	0.56	0.53	12 677
1501	2.47	2.10	50 019
1501	1.27	1.17	27 918
1507	0.44	0.49	11 689
1575	46.37	43.01	1 023 600
1585	8.91	8.77	208 660
1643	1.60	1.51	36 046
1653	1.89	2.53	60 101
Total	98.97	98.39	

The sum of percent values over all normal modes is 100. We report results only for modes with strong enough electron–phonon and Raman intensity (relative electron–phonon coupling larger than 0.05%).

The $\mathcal{R}$-coordinate is defined by a set of collective interdependent nuclear displacements, which may be evaluated as shown in the following. We may look for a relation of $\mathcal{R}$ with the displacement between ground and excited state minima, as carried out in the past for defining $\mathcal{R}$ in π-conjugated systems (see the work of Castiglioni *et al.*[2] and the references therein). Within harmonic approximation, the excited state energy surface $E_\alpha(\mathbf{x})$ can be expanded around the minimum of the ground state (i.e. at the FC point):

$$E_\alpha(\mathbf{x}) = E_g^0 + \hbar\Omega_{g\alpha}^0 + \sum_i g_i^\alpha\, x_i + \frac{1}{2}\sum_{ij} f_{ij}^\alpha\, x_i x_j \qquad (6)$$

where $g_i^\alpha = \left\langle \alpha \left| \frac{\partial H}{\partial x_i} \right| \alpha \right\rangle$ is the gradient of the excited state energy surface at the FC point and, similarly, f_{ij}^α are the matrix elements of the Hessian of the excited state energy surface; $\hbar\Omega_{g\alpha}^0$ is the vertical transition energy. The minimum of the excited state surface satisfies $\partial E_\alpha/\partial x_i = 0$; hence, its 'multi-dimensional' distance $\{x_i\}$ from the FC point has to satisfy the following equation:

$$g_i^\alpha + \sum_j f_{ij}^\alpha\, x_j = 0 \qquad (7)$$

The solution to Eqn (7) defines the displacement from the FC point to the excited state minimum or, equivalently, the distance of ground and excited state minima $\Delta x_i^{g\to\alpha}$, that is,

$$x_i = \Delta x_i^{g\to\alpha} = -\sum_j \left(f^{-1}\right)_{ij}^\alpha\, g_j^\alpha \qquad (8)$$

Or equivalently

$$g_i^\alpha = -\sum_j f_{ij}^\alpha\, \Delta x_j^{g\to\alpha} \qquad (9)$$

In vector notation, $\mathbf{g}^\alpha = -\mathbf{f}^\alpha \Delta\mathbf{x}^{g\to\alpha}$. If one considers the unit vectors associated to the two quantities ($\mathbf{g}^\alpha$, $\Delta\mathbf{x}^{g\to\alpha}$), one obtains a collective nuclear displacement suitable for defining the $\mathcal{R}$-coordinate of the π-conjugated system. On the basis of Eqn (9), one concludes that $\mathbf{g}^\alpha$ or $\Delta\mathbf{x}^{g\to\alpha}$ essentially provides the same displacement coordinate when the force constant matrix $\mathbf{f}^\alpha$ does not induce any substantial 'rotation' to the direction of $\Delta\mathbf{x}^{g\to\alpha}$ vector. This happens when $\mathbf{g}^\alpha$ or $\Delta\mathbf{x}^{g\to\alpha}$ is close enough to some eigenvector of the $\mathbf{f}^\alpha$ matrix. The situation for β-carotene has been checked with time-dependent DFT calculations carried out on the lowest dipole-allowed excited state $|\alpha\rangle$. The gradient at the FC point, the optimized structure and the 'force constant matrix' of the excited state have been computed with TD-B3LYP/6-31G** method, providing $\Delta\mathbf{x}^{g\to\alpha}$, $\mathbf{g}^\alpha$ and $\mathbf{f}^\alpha$.

The direct comparison of $\Delta\mathbf{x}^{g\to\alpha}$ with $\mathbf{g}^\alpha$ is potentially plagued with spurious roto-translations or large amplitude motions of the molecule upon excitation, which hinder the straightforward evaluation of the vibrational contribution to $\Delta\mathbf{x}^{g\to\alpha}$. Hence, we adopt an indirect approach, which consists in considering Eqn (9) and checking whether the components of normalized $\mathbf{g}^\alpha$ ($\mathbf{u}_\mathcal{R}$) are close to those of some eigenvector of the $\mathbf{f}^\alpha$ matrix, i.e. we

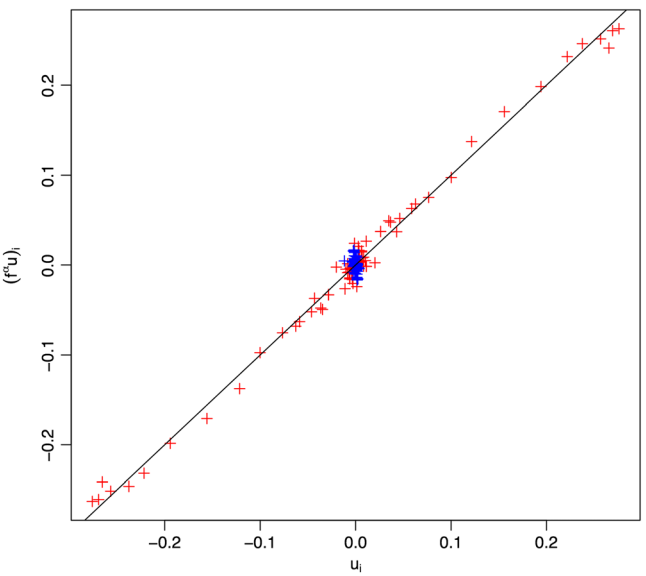

Figure 2. Correlation between the components of the normalized $\mathcal{R}$ vector ($\mathbf{u}_\mathcal{R} = \mathbf{g}/\|\mathbf{g}\|$) and those of the normalized vector obtained from the matrix product $\mathbf{f}^\alpha\mathbf{u}_\mathcal{R}$ (from TD-B3LYP/6-31G** calculations). Red points indicate the components of the vectors pertaining to carbon atoms, while blue points are relative to hydrogen atoms, which are unaffected by a displacement along the $\mathcal{R}$-coordinate. This figure is available in colour online at wileyonlinelibrary.com/journal/jrs

checked if $\mathbf{u}_{\mathcal{R}}$ is parallel to $\mathbf{f}^{\alpha}\mathbf{u}_{\mathcal{R}}$. Figure 2 shows the components of the unit vector defining the ECC coordinate, $\mathbf{u}_{\mathcal{R}}$, against the components of the vector $\mathbf{f}^{\alpha}\mathbf{u}_{\mathcal{R}}$ (normalized as well). It is clear that the two vectors are parallel to a good approximation; hence, the gradient $\mathbf{g}^{\alpha}$ ($\mathcal{R}$-coordinate) is very close to an eigenvector of the force constant in the excited state. In conclusion, on the basis of Eqn (9) and the results summarized in Fig. 2, we deduce that for the lowest lying bright state of β-carotene, the gradient $\mathbf{g}^{\alpha}$ and the displacement $\Delta\mathbf{x}^{g\rightarrow\alpha}$ are parallel vectors, to a good approximation. Thus, in principle, both quantities can be used to define the $\mathcal{R}$-coordinate, i.e. one can either calculate the gradient at the FC point or optimize the excited electronic state and compute the geometry difference with respect to the ground state. These two approaches can be used to define the $\mathcal{R}$-coordinate in other carotenoids and oligoenes and in general in other molecular systems.

Raman scattering

The aforementioned discussion has highlighted the key role of electron–phonon coupling in resonant Raman spectroscopy of π-conjugated molecules. We consider now the expressions given in the work of Nafie *et al.*[5] for resonant Raman intensities of overtones and combinations. We aim at providing working equations suitable for numerical evaluation, on the basis of quantities directly obtained from quantum chemical calculations. Neglecting the contributions from hot band transitions and anti-Stokes processes and assuming that the interaction process consists in the creation of n vibrational quanta, each one with energy $\hbar\Omega$, in n successive steps (promoted by time-ordered radiation field–molecule interaction by the first-order perturbative terms of Eqns (1–5) and as presented in the first two schemes of Fig. 3(a)[5,9]), the Raman intensity of a generic n-th overtone of a given normal mode Q can be written as follows:

$$I_n \propto |\langle 0|Q|1\rangle\langle 1|Q|2\rangle \ldots \langle n-1|Q|n\rangle|^2 \times \left| \frac{\langle g|\mu_2|\alpha\rangle \left\langle \alpha \left| \frac{\partial H}{\partial Q} \right| \alpha \right\rangle^n \langle \alpha|\mu_1|g\rangle}{\prod_{k=0}^{n}\left(E_\alpha - E_g - \hbar\omega_1 + k\hbar\Omega + i\Gamma\right)} \right|^2 \tag{10}$$

In the work of Nafie *et al.*,[5] it is shown how the denominator of Eqn (10) stems from the use of time-ordered diagrams in the context of perturbation theory describing vibronic interactions[7] through $(\partial H/\partial Q)_0 Q$ (i.e. Herzberg–Teller). Hence, the unperturbed energy differences $(E_\alpha - E_g)$ are the vertical transition energies computed at the unperturbed nuclear equilibrium of the ground state ($Q=0$). Dimensional analysis of the right-hand term of Eqn (10) reveals a quantity commensurate to the square of a polarizability (i.e. the square of a transition dipole moment squared, divided by an energy). This is expected on the basis of the general quantum expression for Raman scattering (Kramers–Heisenberg–Dirac) given, for instance, in the work of Albrecht[10]:

$$I_{i\rightarrow f} = \frac{2^7\pi^5}{3^2c^4} I_0 (\nu_0 + \nu_i - \nu_f)^4 \sum_{\rho\sigma} \left| \left[\alpha_{\rho\sigma}\right]_{i\rightarrow f} \right|^2 \tag{11}$$

The quantum mechanical term $[\alpha_{\rho\sigma}]_{i\rightarrow f}$ directly relates to molecular vibrational and electronic structure (i.e. resonances) and dimensionally corresponds to a polarizability. Its expression involves the product of transition dipole moments divided by transition energies.

The square of the product of integrals over vibrational wavefunctions in Eqn (10), i.e. $|\prod_{k=1..n}\langle k-1|Q|k\rangle|^2$, can be evaluated within mechanical harmonic approximation by means of popular tables of integrals involving Hermite polynomials, as those given in the study of Wilson *et al.*.[11] The result is

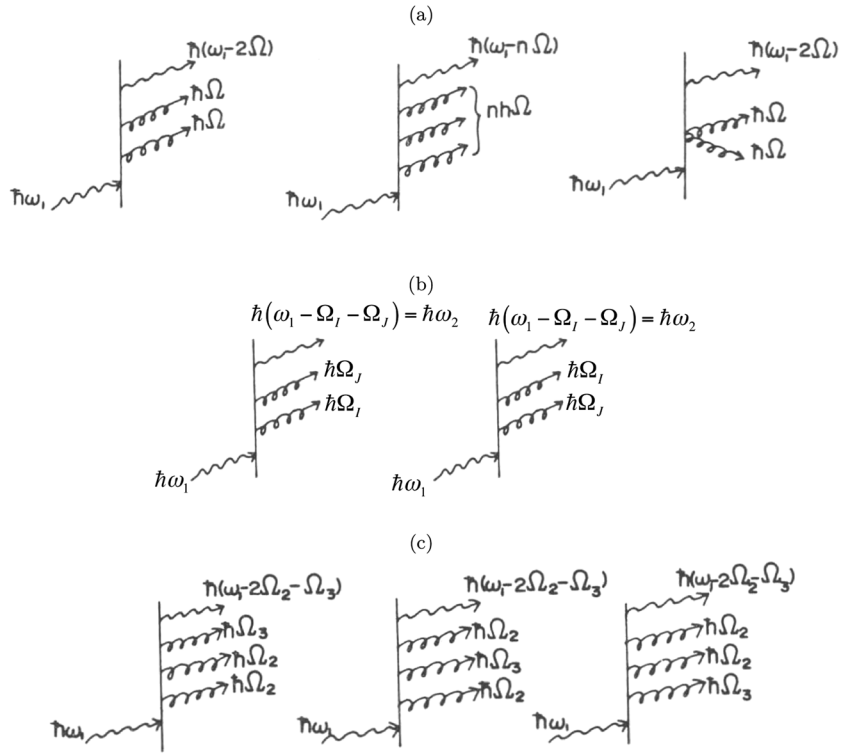

Figure 3. Time-ordered diagrams relative to Raman process involving (a) overtones of a given mode Q; (b) combination of two modes Q_I and Q_J; and (c) three-quanta combinations over two normal modes. Diagrams have been taken and adapted from the study of Nafie *et al.*[5]

$n!\left(\frac{\hbar}{2\Omega}\right)^n$ (details are given in Appendix A), so that the expression given by Eqn (10) can be written as follows:

$$I_n \propto n!\left(\frac{\hbar}{2\Omega}\right)^n \times \left|\frac{\langle g|\mu_2|\alpha\rangle\left\langle\alpha\left|\frac{\partial H}{\partial Q}\right|\alpha\right\rangle^n\langle\alpha|\mu_1|g\rangle}{\prod_{k=0}^{n}\left(E_\alpha - E_g - \hbar\omega_1 + k\hbar\Omega + i\Gamma\right)}\right|^2 \tag{12}$$

By following the illustration of the time-ordered diagrams given in the work of Nafie *et al.*,[5] one can also derive expressions for Raman intensities associated with combination Raman processes involving normal modes Q_I and Q_J. The two leading diagrams are given in Fig. 3(b). Their evaluation provides the following result:

$$I_{I+J} \propto |<0|Q_I|1><0|Q_J|1>|^2 \times \left|\begin{array}{c}\frac{\langle g|\mu_2|\alpha\rangle\left\langle\alpha\left|\frac{\partial H}{\partial Q_I}\right|\alpha\right\rangle\left\langle\alpha\left|\frac{\partial H}{\partial Q_J}\right|\alpha\right\rangle\langle\alpha|\mu_1|g\rangle}{\left(E_\alpha - E_g - \hbar\omega_1 + i\Gamma\right)\left(E_\alpha - E_g - \hbar\omega_1 + \hbar\Omega_I + i\Gamma\right)\left(E_\alpha - E_g - \hbar\omega_1 + \hbar\Omega_I + \hbar\Omega_J + i\Gamma\right)} \\ + \frac{\langle g|\mu_2|\alpha\rangle\left\langle\alpha\left|\frac{\partial H}{\partial Q_J}\right|\alpha\right\rangle\left\langle\alpha\left|\frac{\partial H}{\partial Q_I}\right|\alpha\right\rangle\langle\alpha|\mu_1|g\rangle}{\left(E_\alpha - E_g - \hbar\omega_1 + i\Gamma\right)\left(E_\alpha - E_g - \hbar\omega_1 + \hbar\Omega_J + i\Gamma\right)\left(E_\alpha - E_g - \hbar\omega_1 + \hbar\Omega_J + \hbar\Omega_I + i\Gamma\right)}\end{array}\right|^2 \tag{13}$$

which simplifies to

$$I_{I+J} \propto \left(\frac{\hbar}{2\Omega_I}\right)\left(\frac{\hbar}{2\Omega_J}\right) \times \left|\begin{array}{c}\frac{\langle g|\mu_2|\alpha\rangle\left\langle\alpha\left|\frac{\partial H}{\partial Q_I}\right|\alpha\right\rangle\left\langle\alpha\left|\frac{\partial H}{\partial Q_J}\right|\alpha\right\rangle\langle\alpha|\mu_1|g\rangle}{\left(E_\alpha - E_g - \hbar\omega_1 + i\Gamma\right)\left(E_\alpha - E_g - \hbar\omega_1 + \hbar\Omega_I + i\Gamma\right)\left(E_\alpha - E_g - \hbar\omega_1 + \hbar\Omega_I + \hbar\Omega_J + i\Gamma\right)} \\ + \frac{\langle g|\mu_2|\alpha\rangle\left\langle\alpha\left|\frac{\partial H}{\partial Q_J}\right|\alpha\right\rangle\left\langle\alpha\left|\frac{\partial H}{\partial Q_I}\right|\alpha\right\rangle\langle\alpha|\mu_1|g\rangle}{\left(E_\alpha - E_g - \hbar\omega_1 + i\Gamma\right)\left(E_\alpha - E_g - \hbar\omega_1 + \hbar\Omega_J + i\Gamma\right)\left(E_\alpha - E_g - \hbar\omega_1 + \hbar\Omega_J + \hbar\Omega_I + i\Gamma\right)}\end{array}\right|^2 \tag{14}$$

Evaluation of resonant Raman intensities of β-carotene

To numerically evaluate relative Raman intensities for fundamentals, overtones and combinations, we simplify the aforementioned expressions, assuming resonance condition, $\hbar\omega_1 \approx E_\alpha - E_g$, and factoring out transition dipoles. Furthermore, $\langle\alpha|\partial H/\partial Q_k|\alpha\rangle = \mathbf{g}\cdot\mathbf{L}_k$, where $\mathbf{g}$ is the gradient at the FC point on the excited state relevant for the resonance condition and $\mathbf{L}_k$ are the nuclear displacements associated to the normal coordinate Q_k. For fundamental Raman transitions, this gives the following:

$$I_k \propto \frac{\hbar}{2\Omega_k}\left|\frac{\mathbf{g}\cdot\mathbf{L}_k}{i\Gamma(i\Gamma + \hbar\Omega_k)}\right|^2 = \frac{1}{2\hbar\Omega_k}\left|\frac{\hbar\mathbf{g}\cdot\mathbf{L}_k}{i\Gamma(i\Gamma + \hbar\Omega_k)}\right|^2 \tag{15}$$

For overtones (first two schemes in Fig. 3(a)),

$$\begin{aligned} I_{nk} &\propto n!\left(\frac{\hbar}{2\Omega_k}\right)^n\left|\frac{(\mathbf{g}\cdot\mathbf{L}_k)^n}{\prod_{l=0\,..n}(i\Gamma + l\hbar\Omega_k)}\right|^2 = \\ &= n!\left(\frac{1}{2\hbar\Omega_k}\right)^n\left|\frac{(\hbar\mathbf{g}\cdot\mathbf{L}_k)^n}{\prod_{l=0\,..n}(i\Gamma + l\hbar\Omega_k)}\right|^2 \end{aligned} \tag{16}$$

For combination of two quanta over two normal modes (Q_h and Q_k), one has (Fig. 3(b))

$$\begin{aligned} I_{h+k} \propto &\left(\frac{\hbar}{2\Omega_h}\right)\left(\frac{\hbar}{2\Omega_k}\right) \times \left|\frac{(\mathbf{g}\cdot\mathbf{L}_h)(\mathbf{g}\cdot\mathbf{L}_k)}{i\Gamma(i\Gamma + \hbar\Omega_h)(i\Gamma + \hbar\Omega_h + \hbar\Omega_k)}\right. \\ &\left. + \frac{(\mathbf{g}\cdot\mathbf{L}_k)(\mathbf{g}\cdot\mathbf{L}_h)}{i\Gamma(i\Gamma + \hbar\Omega_k)(i\Gamma + \hbar\Omega_k + \hbar\Omega_h)}\right|^2 = \\ &= \left(\frac{1}{2\hbar\Omega_h}\right)\left(\frac{1}{2\hbar\Omega_k}\right) \\ &\times \left|\frac{(\hbar\mathbf{g}\cdot\mathbf{L}_h)(\hbar\mathbf{g}\cdot\mathbf{L}_k)}{i\Gamma(i\Gamma + \hbar\Omega_h)(i\Gamma + \hbar\Omega_h + \hbar\Omega_k)}\right. \\ &\left. + \frac{(\hbar\mathbf{g}\cdot\mathbf{L}_k)(\hbar\mathbf{g}\cdot\mathbf{L}_h)}{i\Gamma(i\Gamma + \hbar\Omega_k)(i\Gamma + \hbar\Omega_k + \hbar\Omega_h)}\right|^2 \end{aligned} \tag{17}$$

Three quanta Raman transitions over two normal modes (Q_h and Q_k) (Fig. 3(c)) give rise to

$$\begin{aligned} I_{h+2k} \propto 2&\left(\frac{1}{2\hbar\Omega_h}\right)\left(\frac{1}{2\hbar\Omega_k}\right)^2\left|(\hbar\mathbf{g}\cdot\mathbf{L}_h)(\hbar\mathbf{g}\cdot\mathbf{L}_k)^2\left[\frac{1}{i\Gamma(i\Gamma + \hbar\Omega_h)(i\Gamma + \hbar\Omega_h + \hbar\Omega_k)(i\Gamma + \hbar\Omega_h + 2\hbar\Omega_k)}\right.\right. \\ &\left.\left. + \frac{1}{i\Gamma(i\Gamma + \hbar\Omega_k)(i\Gamma + 2\hbar\Omega_k)(i\Gamma + \hbar\Omega_h + 2\hbar\Omega_k)} + \frac{1}{i\Gamma(i\Gamma + \hbar\Omega_k)(i\Gamma + \hbar\Omega_k + \hbar\Omega_h)(i\Gamma + \hbar\Omega_h + 2\hbar\Omega_k)}\right]\right|^2 \end{aligned} \tag{18}$$

Three quanta Raman transitions over three normal modes (Q_h, Q_k and Q_l) (scheme not reported) give rise to

$$I_{h+k+l} \propto \left(\frac{1}{2\hbar\Omega_h}\right)\left(\frac{1}{2\hbar\Omega_k}\right)\left(\frac{1}{2\hbar\Omega_l}\right) \times \Big|(\hbar\mathbf{g}\cdot\mathbf{L}_h)(\hbar\mathbf{g}\cdot\mathbf{L}_k)(\hbar\mathbf{g}\cdot\mathbf{L}_l)\Big[\frac{1}{i\Gamma(i\Gamma+\hbar\Omega_h)(i\Gamma+\hbar\Omega_h+\hbar\Omega_k)(i\Gamma+\hbar\Omega_h+\hbar\Omega_k+\hbar\Omega_l)}$$
$$+\frac{1}{i\Gamma(i\Gamma+\hbar\Omega_h)(i\Gamma+\hbar\Omega_h+\hbar\Omega_l)(i\Gamma+\hbar\Omega_h+\hbar\Omega_l+\hbar\Omega_k)}$$
$$+\frac{1}{i\Gamma(i\Gamma+\hbar\Omega_k)(i\Gamma+\hbar\Omega_k+\hbar\Omega_h)(i\Gamma+\hbar\Omega_k+\hbar\Omega_h+\hbar\Omega_l)} \quad (19)$$
$$+\frac{1}{i\Gamma(i\Gamma+\hbar\Omega_k)(i\Gamma+\hbar\Omega_k+\hbar\Omega_l)(i\Gamma+\hbar\Omega_k+\hbar\Omega_l+\hbar\Omega_h)}$$
$$+\frac{1}{i\Gamma(i\Gamma+\hbar\Omega_l)(i\Gamma+\hbar\Omega_l+\hbar\Omega_h)(i\Gamma+\hbar\Omega_l+\hbar\Omega_h+\hbar\Omega_k)}$$
$$+\frac{1}{i\Gamma(i\Gamma+\hbar\Omega_l)(i\Gamma+\hbar\Omega_l+\hbar\Omega_k)(i\Gamma+\hbar\Omega_l+\hbar\Omega_k+\hbar\Omega_h)}\Big]\Big|^2$$

Dimensional analysis reveals that $\hbar\mathbf{g}\cdot\mathbf{L}_k$ has units of [energy$^{3/2}$].[2] By consequence, the dimensions of the right-hand-side of Eqns (15–19) are all [energy^{-2}], as expected on the basis of the discussion that closely follows Eqn (10).

By making use of Eqns (15–19), on the basis of results from DFT calculations (as mentioned earlier), we have computed resonant Raman intensities of fundamentals, overtones and combinations of β-carotene. These data have been used to produce a simulated Raman spectrum, which is reported in Fig. 4 and compared with experimental data taken from the study of Okamoto *et al.*[1]

Discussion of the results and conclusions

The results of Fig. 4 are pretty encouraging for two reasons:

1. Within each one of the four manifolds of Raman resonant features defined by Okamoto *et al.*,[1] the agreement between experiments and theory/computations is pretty good (looking at Fig. 4, the manifolds contain respectively the following: the fundamentals, between 1000 and 1600 cm^{-1}; the first overtones ($2\nu_i$) plus two-quanta combinations, between 2000 and 3200 cm^{-1} a set of higher-order combinations involving three quanta, between 3200 and 4200 cm^{-1}; and the second overtone of ν_1 ($3\nu_1$) plus other combinations, between 4200 and 5000 cm^{-1}).
2. Most importantly, these nice results are arrived at by just calculating the gradient g or other associated quantities such as $u_{\mathcal{R}}$, which means that a common mechanism for electron–phonon coupling explains the majority of intensity data of Fig. 4, and what really counts to confer intensity to fundamental, overtone or combination features in resonance Raman spectra is the participation of the $\mathcal{R}$-coordinate in the normal modes involved in the transitions under observation.

However, looking more closely, one realizes that the agreement of theory to experiment is not 100% perfect, and this will require some further effort to obtain an impeccable interpretation of the data. As a first step in this direction, we may notice that the features observed at 3048, 3319 and 4050 cm^{-1} are underestimated by the present calculations. The first and last bands are attributed to $2\nu_1$ and to $2\nu_1+\nu_4$, respectively. A possible source of error in the evaluation of intensities is the neglect in our approach of one basic interaction event included in

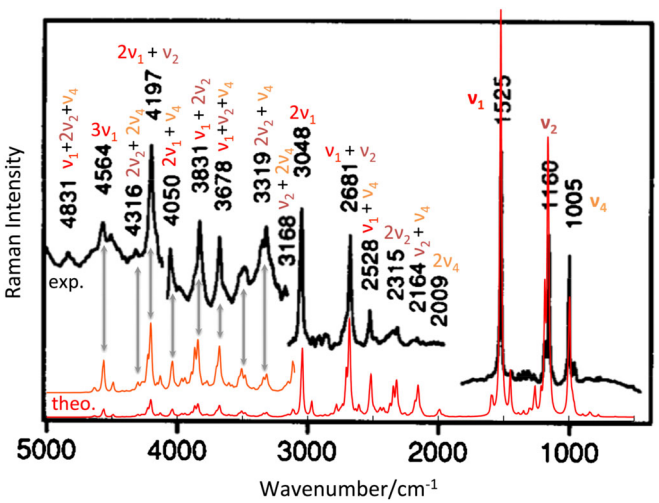

Figure 4. Resonant Raman spectrum of β-carotene. Comparison of experimental data recorded by Okamoto *et al.*[1] with excitation at 457.9 nm (black line) and calculated data by the present theoretical analysis (red and orange lines). Wave numbers from DFT have been scaled by 0.965; strict mechanical harmonic approximation has been used to compute the wavenumbers of overtones and combinations based on fundamentals. Γ value for numerical calculations of Raman intensities is 250 cm^{-1} (the pattern of relative Raman intensities does not sensibly change for $\Gamma < 1000$ cm^{-1}). The orange line shows the simulated Raman spectrum magnified four times. Assignment of overtones and combinations follows the one given in the study of Okamoto *et al.*[2] The experimental peak at 4831 cm^{-1} is not present in the simulations because we have not considered here fourth-order Raman processes. This figure is available in colour online at wileyonlinelibrary.com/journal/jrs

[2]This is easily proved because Cartesian displacements along the k-th normal mode satisfy $\Delta\mathbf{x}_k = \mathbf{L}_k\Delta Q_k$ and the normal coordinate Q_k is mass-weighted and hence has dimension of [length · mass$^{1/2}$]. Hence, $\mathbf{L}_k$ has dimension of [mass$^{-1/2}$].

the original derivation of Nafie *et al.*,[5] namely the one involving the direct generation of an overtone vibration, which we recall in Fig. 3(a), last column, pasting the picture from Nafie *et al.* [5] The intensity associated to such event in resonance condition ($\hbar\omega_1 = E_\alpha - E_g$) is

$$I_{2k} \propto \left|\langle 0|Q_k^2|2\rangle\right|^2 \frac{1}{4}\left|\frac{\langle g|\mu_2|\alpha\rangle\left\langle\alpha\left|\frac{\partial^2 H}{\partial Q_k^2}\right|\alpha\right\rangle\langle\alpha|\mu_1|g\rangle}{i\Gamma(i\Gamma + 2\hbar\Omega_k)}\right|^2 \qquad (20)$$

Indeed, in the time-ordered scheme, such term arises because of a first-order event (such as the one promoting fundamentals) and is caused by second-order perturbative interaction, $\frac{1}{2}\frac{\partial^2 H}{\partial Q_k^2} Q_k^2$.[9] The numerator of the last factor in Eqn (20) contains the square of the vibrational energy of mode Q_k in the electronic excited state $|\alpha\rangle$, which we may indicate as $\hbar\Omega'_k$. Comparison of Eqn (16) for $n = 2$ and of Eqn (20) shows that the two terms are in the following ratio:

$$\frac{I_{eq.20}}{I_{eq.16}} = \frac{1}{4}\left[\frac{\hbar\Omega'_k}{\hbar\mathbf{g}\cdot\mathbf{L}_k}\right]^4 |\hbar\Omega_k + i\Gamma|^2 \qquad (21)$$

This means that the importance of the neglected term increases with Ω_k, which may explain why ν_1 overtones and combination involving ν_1, the largest in the spectrum of the fundamental manifold, should have a larger intensity than estimated in the present model.

Because of the theoretical model we have presented earlier, we recognize that the observation of Raman overtones in resonance conditions is not typical of β-carotene. Indeed, not only Tasumi's group did observe the same phenomenon in Raman spectra of other π-conjugated and variously substituted or terminated polyenes[1] but also Ci *et al.*[12] studied hexatriene and found that, by progressively tuning to resonance the excitation radiation, overtone features increase in Raman intensity more evidently than fundamentals.

For this reason, we applied the Nafie–Stein–Peticolas theory also to hexatriene, with excellent results, as reported in the Supporting information.

Furthermore, the results presented here can find application to other systems than carotenoids, for which electron–phonon processes are relevant as, for instance, carbon nanotubes and graphene.[13,14]

The fact that the intensities of the overtones can be easily recorded in resonance condition may be rationalized by simple DFT calculations reported in Fig. 5 (for the sake of consistency with the rest of this work, we kept B3LYP/6-31G** level of theory). There, we demonstrate that divergences in the trace of the polarizability tensor of hexatriene, because of resonance with radiation of wavelength in the interval 240–290 nm, are met with displacements along the strongest Raman active CC stretching mode (TD-B3LYP/6-31G** locates resonance with S_1 at about 255 nm). Because overtones imply large displacements, these calculations further justify the special connection of overtones to resonance. In fact, large amplitude displacements ΔQ, when close to resonance conditions, allow probing the whole singular region in the $\alpha(Q)$ diagram (Figure 5). In a polarizability derivative context for Raman intensity, this would imply exploring a region where the linear approximation $\alpha(Q) \approx \alpha_0 + (\partial\alpha/\partial Q)_0 Q$ is no more tenable; hence, overtones due to higher polarizability derivatives would be straightforwardly implied.

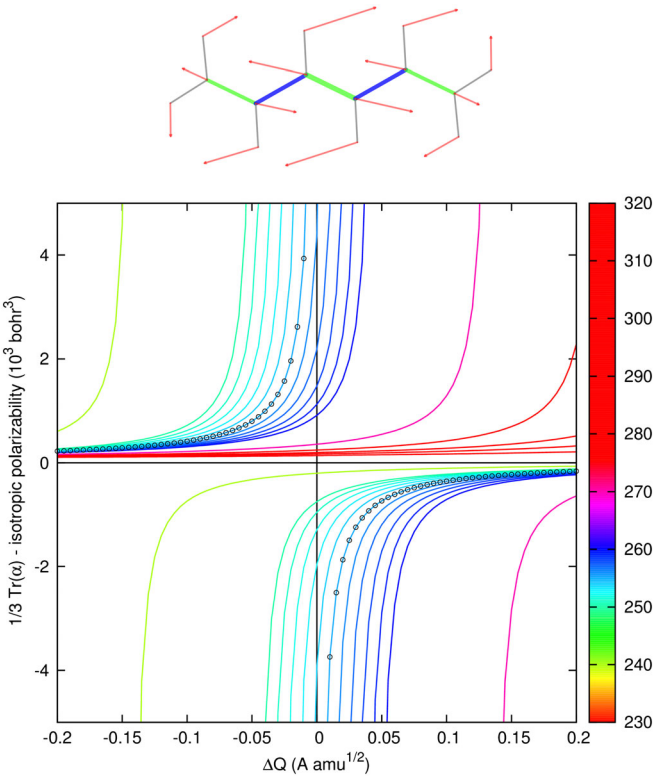

Figure 5. Calculated value of isotropic polarizability of hexatriene *versus* the displacement ΔQ along the strongest Raman mode (computed at 1708 cm^{-1}; nuclear displacement pattern reported at the top of figure) in presence of electromagnetic field of wavelength in the interval 200–600 nm (B3LYP/6-31G** calculations). Units of the color bar are nanometer. The data corresponding to the resonance predicted by TD-B3LYP/6-31G** (255 nm) are plotted with open circle symbols. For the sake of understanding, at the maximum displacement ΔQ of +0.2 A/amu$^{1/2}$, the central C–C bond elongates from its equilibrium value of 1.352 Å to the value of 1.408 Å. This figure is available in colour online at wileyonlinelibrary.com/journal/jrs

Appendix: A

By referring to the well-known integrals over the eigenfunctions of the harmonic oscillator (see, for instance, the work of Wilson *et al.*[11]), it is straightforward to derive the following result:

$$\begin{aligned}\langle 0|Q|1\rangle\langle 1|Q|2\rangle\ldots\langle n-1|Q|n\rangle = \\ = \prod_{k=0\,..(n-1)} \langle k|Q|k+1\rangle = \\ = \prod_{k=0\,..(n-1)} \left[\frac{\hbar}{2\Omega}(k+1)\right]^{1/2}\end{aligned} \qquad (A1)$$

Hence, the square of the modulus becomes

$$\begin{aligned}&|<0|Q|1><1|Q|2> \ldots <n-1\,|Q|n>|^2 = \\ &= \prod_{k=0\,..(n-1)} \left[\frac{\hbar}{2\Omega}(k+1)\right] = \left(\frac{\hbar}{2\Omega}\right)^n \prod_{k=0\,..(n-1)} (k+1) = \\ &= \left(\frac{\hbar}{2\Omega}\right)^n 1\times 2\times\ldots\times(n-1)\times n = n!\left(\frac{\hbar}{2\Omega}\right)^n\end{aligned} \qquad (A2)$$

Acknowledgements

We acknowledge Prof. Mitsuo Tasumi for his helpful discussion regarding data of Okamoto *et al.*[1] We also thank Dr Luigi Brambilla for the FT-Raman spectrum of β-carotene reported in

Fig. 1. M. T. thanks the Italian MIUR for the financial support, under the auspices of the FIRB program RBFR08XH0H (Futuro in Ricerca 2008). G. L. and S. A. thank CARIPLO foundation for funds through the grant 2012–2014 for the program 'Inherently Chiral Multifunctional Conducting Polymers'.

References

[1] H. Okamoto, Y. Sekimoto, M. Tasumi, *Spectrochimica Acta* **1994**, *50A*, 1467.
[2] C. Castiglioni, M. Tommasini, G. Zerbi, *Phil. Trans. R. Soc. Lond. A* **2004**, *362*, 2425.
[3] B. R. Henry, A. W. Tarr, O. S. Mortensen, W. F. Murphy, D. A. C. Compton, *J. Chem. Phys.* **1983**, *79*, 2583.
[4] L. Brambilla, M. Tommasini, G. Zerbi, R. Stradi, *J. Raman Spectrosc.* **2012**, *43*, 1449.
[5] L. A. Nafie, P. Stein, W. L. Peticolas, *Chem. Phys. Lett.* **1971**, *12*, 131.
[6] M. Tommasini, A. Lucotti, G. Zerbi, *J. Raman Spectrosc.* **2011**, *42*, 1207.
[7] W. L. Peticolas, L. A. Nafie, P. Stein, B. Fanconi, *J. Chem. Phys.* **1970**, *52*, 1576.
[8] M. Tommasini, C. Castiglioni, G. Zerbi, *Phys. Chem. Chem. Phys.* **2009**, *11*, 10185.
[9] D. P. Craig, T. Thirunamachandran, Molecular Quantum Electrodynamics, Academic Press, London, **1984**.
[10] A. C. Albrecht, *J. Chem. Phys.* **1961**, *34*, 1476.
[11] E. B. Wilson, J. C. Decius, P. C. Cross, Molecular Vibrations: The Theory of Infrared and Raman Vibrational Spectra, McGraw-Hill, New York, **1955**.
[12] X. Ci, M. A. Pereira, A. B. Myers, *J. Chem. Phys.* **1990**, *92*, 4708.
[13] A. P. Shreve, E. H. Haroz, S. M. Bachilo, R. B. Weisman, S. Tretiak, S. Kilina, S. K. Doorn, *Phys. Rev. Lett.* **2007**, *98*, 037405.
[14] S. Piscanec, M. Lazzeri, F. Mauri, A. C. Ferrari, *Eur. Phys. J. Special Topics* **2007**, *148*, 159.
[15] M. J. Frisch, G. W. Trucks, H. B. Schlegel, G. E. Scuseria, M. A. Robb, J. R. Cheeseman, G. Scalmani, V. Barone, B. Mennucci, G. A. Petersson, H. Nakatsuji, M. Caricato, X. Li, H. P. Hratchian, A. F. Izmaylov, J. Bloino, G. Zheng, J. L. Sonnenberg, M. Hada, M. Ehara, K. Toyota, R. Fukuda, J. Hasegawa, M. Ishida, T. Nakajima, Y. Honda, O. Kitao, H. Nakai, T. Vreven, J. A. Montgomery, Jr., J. E. Peralta, F. Ogliaro, M. Bearpark, J. J. Heyd, E. Brothers, K. N. Kudin, V. N. Staroverov, R. Kobayashi, J. Normand, K. Raghavachari, A. Rendell, J. C. Burant, S. S. Iyengar, J. Tomasi, M. Cossi, N. Rega, J. M. Millam, M. Klene, J. E. Knox, J. B. Cross, V. Bakken, C. Adamo, J. Jaramillo, R. Gomperts, R. E. Stratmann, O. Yazyev, A. J. Austin, R. Cammi, C. Pomelli, J. W. Ochterski, R. L. Martin, K. Morokuma, V. G. Zakrzewski, G. A. Voth, P. Salvador, J. J. Dannenberg, S. Dapprich, A. D. Daniels, O. Farkas, J. B. Foresman, J. V. Ortiz, J. Cioslowski, D. J. Fox, Gaussian 09, Revision A.02, Gaussian, Inc., Wallingford CT, **2009**.

Supporting information

Additional supporting information may be found in the online version of this article at the publisher's web site.